Journal Pre-proof

Seafloor geomorphology of the northern Argentine continental slope at 40-41° S mapped from high-resolution bathymetry

Sebastian Principi, Fermin Palma, Donaldo Mauricio Bran, Graziella Bozzano, José Ignacio Isola, Juan Pablo Ormazabal, Federico Esteban, Luana Acosta, Alejandro Tassone

PII: S0895-9811(23)00560-6

DOI: https://doi.org/10.1016/j.jsames.2023.104748

Reference: SAMES 104748

To appear in: *Journal of South American Earth Sciences*

Received Date: 27 July 2023

Revised Date: 11 November 2023

Accepted Date: 15 December 2023

Please cite this article as: Principi, S., Palma, F., Bran, D.M., Bozzano, G., Isola, José.Ignacio., Ormazabal, J.P., Esteban, F., Acosta, L., Tassone, A., Seafloor geomorphology of the northern Argentine continental slope at 40-41° S mapped from high-resolution bathymetry, *Journal of South American Earth Sciences* (2024), doi: https://doi.org/10.1016/j.jsames.2023.104748.

This is a PDF file of an article that has undergone enhancements after acceptance, such as the addition of a cover page and metadata, and formatting for readability, but it is not yet the definitive version of record. This version will undergo additional copyediting, typesetting and review before it is published in its final form, but we are providing this version to give early visibility of the article. Please note that, during the production process, errors may be discovered which could affect the content, and all legal disclaimers that apply to the journal pertain.

© 2023 Published by Elsevier Ltd.

Seafloor geomorphology of the northern Argentine continental slope at 40-41º S mapped from high-resolution bathymetry

Sebastian Principi[a,b,c], Fermin Palma[a,b,c], Donaldo Mauricio Bran[a,b] , Graziella Bozzano[d,e], José Ignacio Isola[a,f], Juan Pablo Ormazabal[a,b], Federico Esteban[a,b], Luana Acosta[a,b], Alejandro Tassone[a,b].

[a] *CONICET – Universidad de Buenos Aires, Instituto de Geociencias Básicas, Aplicadas y Ambientales de Buenos Aires (IGeBA), Buenos Aires, Argentina*

[b] *Departamento de Ciencias Geológicas, Facultad de Ciencias Exactas y Naturales, Universidad Nacional de Buenos Aires, Argentina*

[c] *YPF Tecnología S.A (Y-TEC), Berisso, Argentina*

[d] *Servicio de Hidrografía Naval (SHN), Buenos Aires, Argentina*

[e] *Consejo Nacional de Investigaciones Científicas y Técnicas (CONICET), Argentina*

[f] *Department of Earth and Planetary Sciences, Rutgers University, Piscataway, NJ, USA*

Corresponding author e-mail address: sebastianprincipi@gl.fcen.uba.ar (Sebastian Principi)

Journal Pre-proof

Abstract

The southern sector of the northern Argentine continental margin (NACM), extending from 40 to 41° S, corresponds to a previously unmapped area of the South Atlantic Ocean in term of high-resolution bathymetry. Newly acquired high resolution data in the slope sector of the NACM between 900 and 5000 meters allowed us to carry out a geomorphological analysis by combining novel multibeam data with a very high-resolution 3D seismic-derived bathymetry. The resultant digital elevation model revealed the presence of a wide variety of seafloor features and allowed us to characterize them by a geomorphometric analysis. Along slope processes, produced by the interaction of contour currents with the seafloor, make up a large array of erosional and

depositional elements on the slope, including a contourite terrace, scours, drift bodies and sediment waves, that as a whole form part of a Contourite Depositional System (CDS). Additionally, across slope processes are also present, and give origin to four deeply incised submarine canyons that intersect the CDS. Overall, this work reveals the geomorphological complexity of this sector of the NACM and serves as a reference point for further studies regarding the sedimentary processes and oceanographic dynamics acting in the continental slope.

Keywords

Seafloor mapping, Marine geomorphology, Submarine canyon, Sediment waves, Contourite drifts, SW Atlantic, Argentine Continental Margin.

1 Introduction

The study of seafloor morphology is crucial for various scientific aspects, including the comprehension of geological and oceanographic processes that impact our planet. Moreover, this knowledge holds great value for practical applications such as the creation of precise hydrographic charts, the development of submarine infrastructure, and the assessment of sites for seafloor mining. In this regard, the acquisition of high-resolution multibeam bathymetry has emerged as a vital step in seafloor mapping, enabling the accurate characterization of seafloor geometry with the necessary spatial resolution for detailed geomorphometric analyses (Gavazzi, 2019). Nevertheless, 80% of our oceans are still unmapped at high resolution.

In this context, the northern Argentine continental margin (NACM), is still a poorly explored region of the South Atlantic Ocean. This subsector spans from the northern boundary of the Argentine continental margin at 36°S up to 42°S; laterally, it extends from the inner edge of the shelf at 10 m depth up to the beginning of with the abyssal plan at 5000 m depth. It can be further divided into northern and southern regions (Figure 1 A), which are marked by the presence of two submarine canyon systems (SCS, Ewing and Lonardi, 1971; Hernández-Molina et al., 2009): the Mar del Plata SCS (36-39°S) and the Bahia Blanca SCS (39-42°S).

These submarine canyons are important elements of the seafloor landscape (Ewing and Lonardi, 1971) that play a key role in shaping marine dynamics by transporting sediment and organic matter from shallow water to deeper water, serving as hotspots for benthic and pelagic communities, and hosting cold-water coral mounds (Daly, 1936; Fernandez-Arcaya et al., 2017; Shepard, 1981, 1972). Nevertheless, the morphology and geometry of these canyons, as well as their interplay with the local bottom currents are still virtually unknown. In this region, active, along-slope oceanic processes interact with the seafloor forming a large Contouritic Depositional System (CDS, Hernández-Molina et al., 2009) that coexists with down-slope sedimentary processes associated to the numerous submarine canyons and to the continental slope instability. This scenario makes the NACM a natural laboratory for studying deep-sea sedimentary processes (Preu et al., 2013; Warratz et al., 2017). Previous studies have addressed some of these topics in the northern part of the NACM (~38°S, Figure 1), using high-resolution bathymetric and seismic profiles (Preu et al., 2013; Steinmann et al., 2020; Warratz et al., 2017; Wilckens et al., 2021). On the contrary, in the southern part of the NACM, between 40 and 41° S, high-resolution bathymetric information is missing, and investigations have been restricted to low-frequency seismic methods (Ercilla et al., 2019; Gruetzner et al., 2016; Loegering et al., 2013, Figure 1). Thus, much of the continental slope morphology of the southern NACM remains unexplored so far.

This work presents the first high-resolution mapping and geomorphometric analysis of the southern sector of the NACM, using a combination of newly acquired multibeam data with bathymetry derived from reflection seismics. The resultant geomorphological map provides new insights into the seafloor morphology along with some hint about past and present sedimentary and oceanographic processes in this sector of the Western South Atlantic Ocean.

2 Geological and oceanographic setting of the study area

The NACM (Figure 1 A) is part of a passive rifted margin, developed during the early Cretaceous following the break-up of Gondwana supercontinent and seafloor spreading of the South Atlantic (Ramos, 1996). It stretches from the continental shelf to the abyssal plain and hosts the Salado and Colorado sedimentary offshore basins.

This region is part of a major CDS, which extends along the entire Argentine continental slope and rise (Hernández-Molina et al., 2009) shaped by the interaction of bottom water masses with the seafloor. The NACM is swept by three water masses of southern origin: Antarctic Intermediate Water (AAIW), Circumpolar Deep Water (CDW) and Antarctic Bottom Deep Water (AABW). The North Atlantic Deep Water (NADW), of northern origin, divides the CDW into two branches, the Upper Circumpolar Deep Water (UCDW) and the Lower Circumpolar Deep Water (LCDW; Reid et al., 1977, Figure 1 B).

In the southern NACM, the CDS is characterized by contouritic drifts, sediment waves and terraces (Ercilla et al., 2019; Gruetzner et al., 2016) and is interrupted by the Bahia Blanca SCS (Bozzano et al., 2017; Hernández-Molina et al., 2009) which is composed of several main and tributary canyons (Ewing and Lonardi, 1971). Additionally, downslope gravitational processes affect the area, disrupting the seafloor in the form of fault scarps and sliding blocks (Gruetzner et al., 2016) originated by slumping episodes (Anka et al., 2014; Loegering et al., 2013) .

Journal Pre-proof

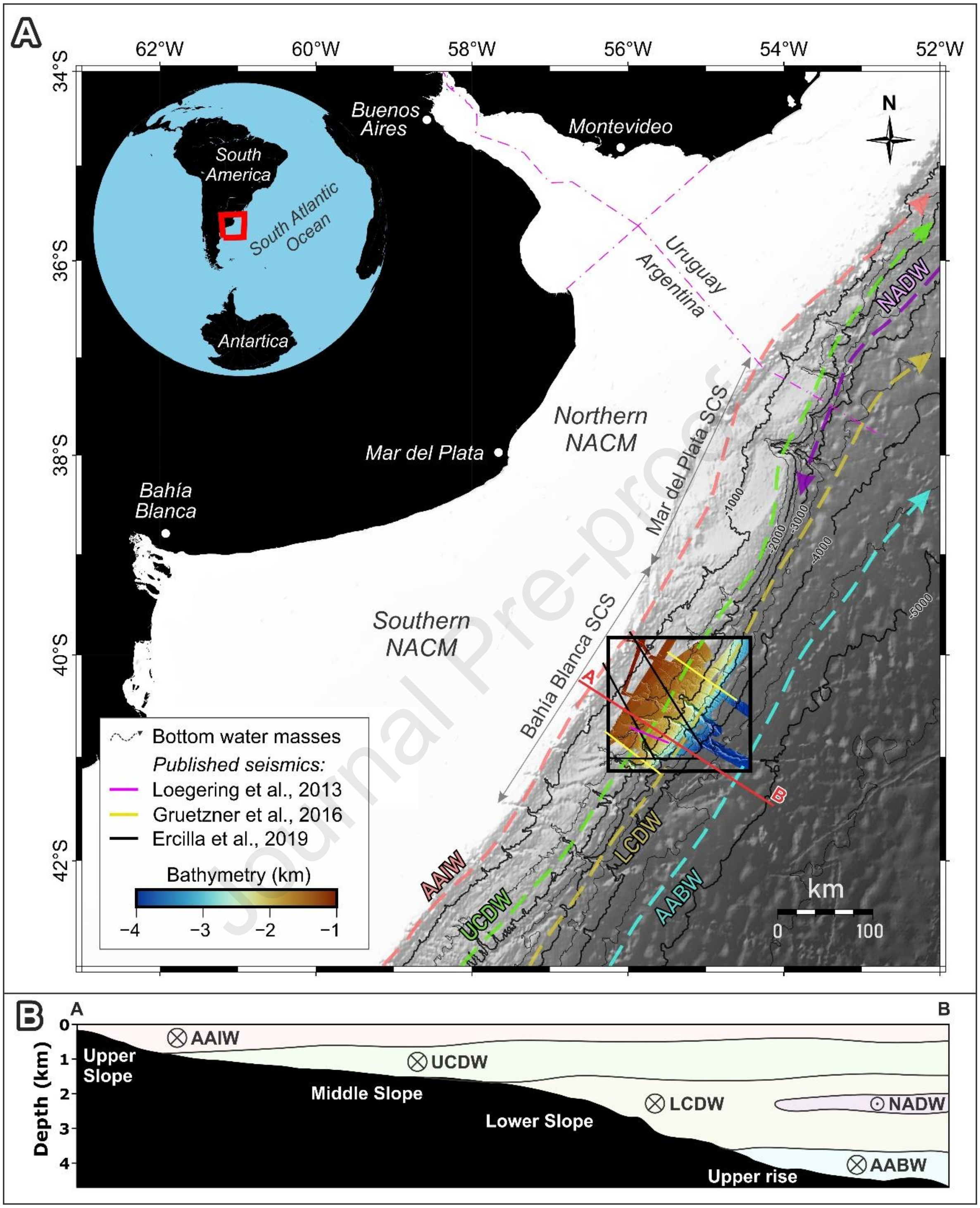

Figure 1: A: Location map of the study area in the NACM. The GEBCO bathymetric model is displayed with a grayscale as a background map. The bathymetric grid used in this work is colored inside the black rectangle, along with the seismic profiles from the literature used for the correlation with the bathymetry. Dashed lines represent the near bottom water masses of the Western South Atlantic (Adapted from Preu et al. 2013*). B: Generalized schematic oceanographic section (A-B) along the northern Argentine continental margin (adapted from* Hernández-Molina et al., 2010 and Piola and Matano, 2001*). NADW: North Atlantic Deep Water; AAIW: Antarctic Intermediate Water, UCDW: Upper Circumpolar Deep Water; LCDW: Lower Circumpolar Deep Water; AABW: Antarctic Bottom Water*

3 Data and Methods

3.1 Multibeam bathymetry processing

High resolution multibeam bathymetric (MBB) data was acquired in 2019 during the YTEC-GTGM-04 survey onboard the R/V Austral (Figure 1). The acquisition was carried out with a hull-mounted Kongsberg EM122 deep sea echosounder, operating at 12 kHz with an opening angle of 140º.

The grid utilized in this study covers an area of 11,000 km^2 and encompasses water depths ranging from 1000 to 5000 meters below sea level (mbsl, Figure 1 A). The processing of the raw data involved georeferencing the files and eliminating any abnormal soundings using Caris HIPS and SIPS v.11.2. This software was also used to generate a 70 x 70m digital elevation model (DEM) using the CUBE gridding algorithm. The resulting DEM was saved as a TIF file and imported into Qgis V3.22 for interpretation. To further refine the DEM, a smoothing algorithm was applied using the r.neighbors module (Shapiro et al., 2019) in GRASS GIS v.7.8.

3.2 Derivation of 3D seismic bathymetry

To enhance the resolution of the existing multibeam bathymetry grid and fill in some of the data gaps, a high-resolution bathymetry was generated using a 3D seismic cube provided by the Ministry of Energy of Argentina. The usage of seismic-derived bathymetry has shown potential in increasing the spatial coverage of high-resolution bathymetric datasets (Power and Clarke, 2019). The seismic data, known as "Colorado 3D", was acquired in 2006 with an inline spacing of 25 m and a crossline spacing of 12.5 m, sampled at intervals of 4 milliseconds. The seismic-derived bathymetry (SDB) was obtained by extracting the first reflection from the seismic data using IHS Kingdom v.2017 software. The resulting seafloor horizon was exported as an XYZ file, which underwent a time-to-depth conversion. Since regional water column velocity profiles were not available, an average velocity of 1500 m/s was utilized to convert the horizon from two-way travel time to depth in meters. The

Journal Pre-proof

converted XYZ file was then gridded and merged with the existing multibeam bathymetry grid using a B-Spline interpolation. This process resulted in a final merged grid with a resolution of 70 x 70 m (Figure 2) that was additionally used to derive a slope gradient map (Figure 3). Areas lacking high-resolution data were filled using the GEBCO grid (GEBCO Bathymetric Compilation Group 2021).

Journal Pre-proof

Journal Pre-proof

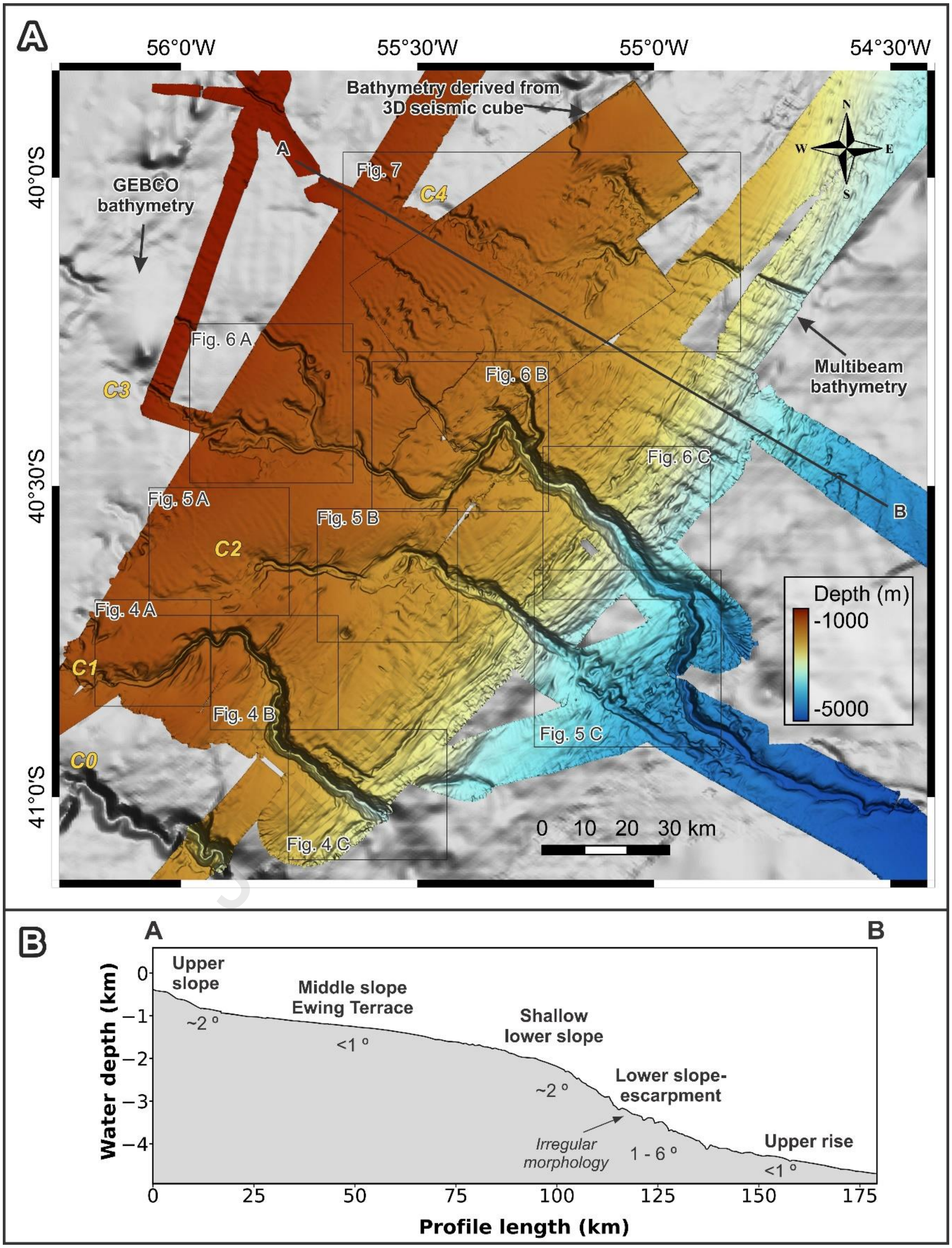

Figure 2: A: Merged bathymetric map of the study area. Black rectangles show the zoom areas of canyons in subsequent figures 4-7. B: profile across the continental margin, showing the physiographic domains of the study area.

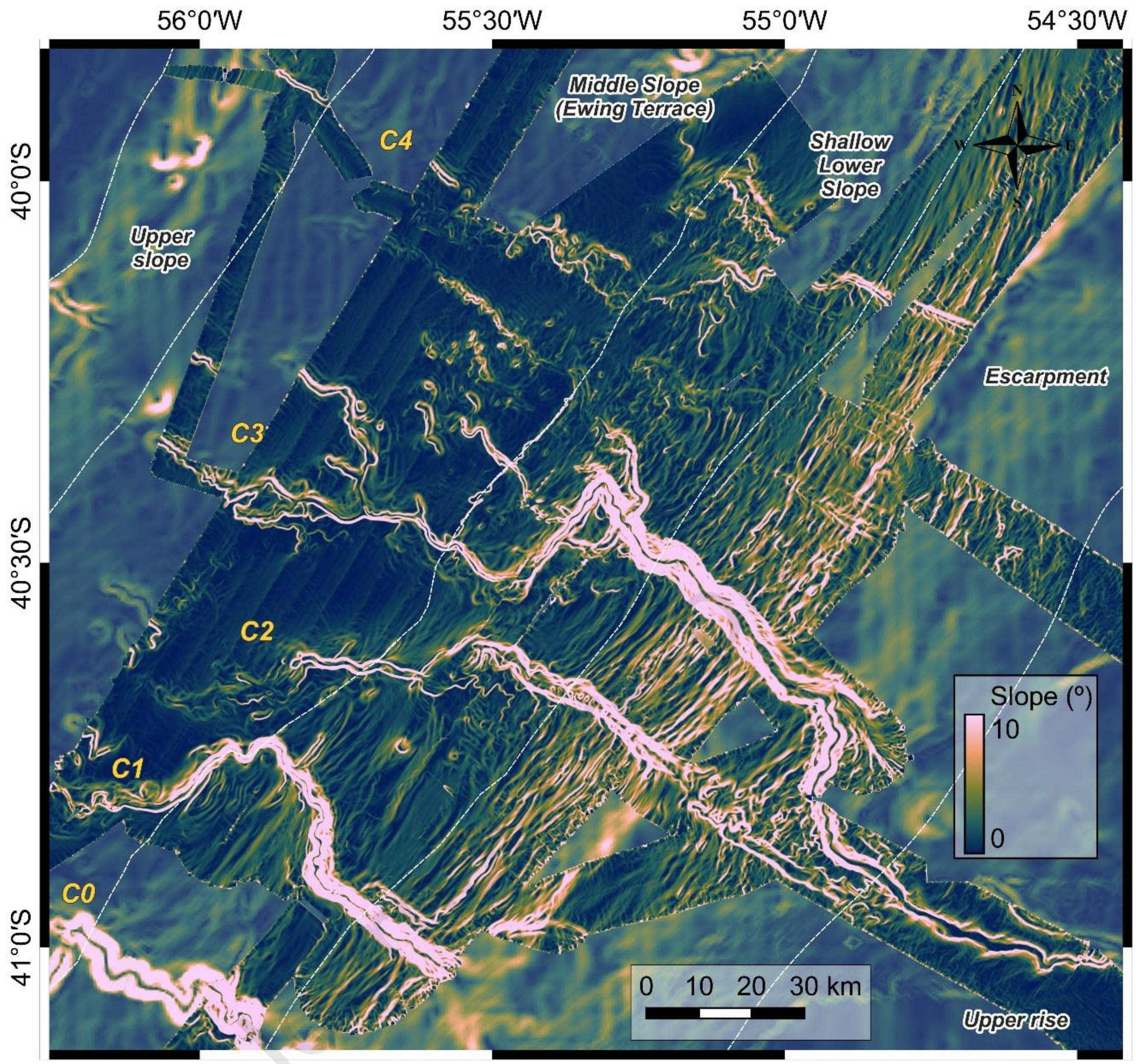

Figure 3: Slope map derived from the merged grid with the four canyons recognized in the study area, labelled C1 to C4. C0 is a partially imaged canyon in the southern sector that is not included in this study.

3.3 Geomorphological analysis

The geomorphological elements were mapped at a 1:125000 scale, using the merged grid in the World Mercator projected coordinate system. We considered the minimum mapping unit to be around 0.5 km^2, which corresponds to 10 contiguous pixels in size. The interpretation was carried out by a combination of visual analysis, calculation of geomorphometric parameters and the creation of bathymetric and slope profiles. To genetically identify the morphological elements within the study area, we rely on previous interpretations based on 2D multichannel seismics (Ercilla et al., 2019; Gruetzner et al., 2016; Loegering et al., 2013, Figure 1 A). To establish a physical correlation between the seismic profiles and the bathymetry, the seismic images were georeferenced into the SEG-Y standard format using the Image2segy software (Farran, 2008). The georeferenced seismic data, along with the merged grid, were incorporated into IHS Kingdom software, enabling the three-dimensional representation of the previously identified features. This integration facilitated a more detailed classification of the features based on their morphological characteristics. The contouritic features and seafloor depressions observed were classified according to the nomenclature proposed by Rebesco et al. (2014) and to the geomorphometric parameters and indices derived from the studies of Isola et al. (2021), Michel et al. (2017) and Schattner (2016). In particular, the depressions were classified based on their ellipticity index, a ratio that quantifies the shape of morphological features by comparing their long axis (the larger diameter along the primary orientation) to their short axis (the smaller diameter perpendicular to the long axis). Submarine canyons of the study area are described based on their cross-sectional profiles, thalweg length, depth, and width range, as well as their orientation changes. To quantify their degree of sinuosity, we employed the sinuosity index (SI), a dimensionless ratio calculated by dividing the canyon length measured along its thalweg and the straight distance between the canyon start and endpoint. A SI of 1 indicates a perfectly straight channel, while moderate (1.3-1.5) and high (>1.5) values indicate increasing degrees of sinuosity (Charlton, 2007).

Journal Pre-proof

4 Results

4.1 Physiography

The study area spans from approximately 900 to 5000 mbsl and includes the continental slope and the upper rise of the NACM (Figure 2 A). The main physiographic domains within this area were determined based on variations in slope gradient and water depth values (Figure 2 B). Specifically, the slope can be divided into three sections: the upper slope, the middle slope (also referred to as "Ewing Terrace"), and the lower slope. The upper slope (~25 km wide) is depicted by relatively high values of the slope gradient (~1-2°) and extends up to 900 mbsl. Here, the upper slope gives rise to the gently dipping (<1°) middle slope. This is the widest of the three domains (~ 70 km), and extends from 900 to 1600 m water depth, covering an area of 6500 km^2. East of the Ewing Terrace, a gradual increase in the topographic gradient (~>1°) marks the progressive transition to the lower slope, which is about 65 km wide. It can be further subdivided into two areas: a shallower sector (shallow lower slope), between 1600 and 2000 mbsl with a ~2° gradient; and a deeper sector, between 2000 and ~4000 mbsl, with a complex slope morphology (here named escarpment). This escarpment displays an irregular topography with variable slope values that fluctuate between 1° to 6°. The upper continental rise, starting beyond 4000 mbsl at the foot of the lower continental slope, is characterized by low relief values (< 1°) and extends eastwards until it merges with the abyssal plain.

4.2 Geomorphological features

The geomorphological analysis allowed us to identify and map the distribution of various features based on their morphological expression, extension, size, orientation and geomorphometric characteristics. Some of these morphologies, such as submarine canyons, are found in different physiographic domains, while others are confined to specific sectors of the continental slope. The following sections provide a detailed description of these identified features, including the

Journal Pre-proof

aforementioned submarine canyons, as well as terraces, scarps, elongated and subcircular depressions, and depositional features.

4.2.1 Submarine canyons

The studied segment of the Bahía Blanca SCS includes four submarine canyons, named here C1-4 (Figure 2 and Figure 3). The southernmost canyon (C0) is not here described since it is marginally imaged by the bathymetric data.

4.2.1.1 Canyon C1

C1 develops between 1300 and 3300 mbsl, spanning the middle and lower slope. It has a thalweg length of 103 kilometers and displays a highly sinuous (sinuosity index of 1.37) main axis with multiple directional changes. Starting from the middle slope, C1 initially follows a E-W trajectory before encountering a sharp bend at 1500 mbsl (Figure 4 A), where it deviates almost SW-NE for 15 kilometers before returning to its original orientation. On the shallow lower slope, the thalweg exhibits a meandering axis with a minor N-S bend near 1800 mbsl (Figure 4 B), and it becomes completely straight in the northeast-southwest direction as it approaches the escarpment (Figure 4 C).

Furthermore, the canyon's cross section displays variations along the thalweg. In the middle slope (Figure 4 A) the valley exhibits a U-shaped profile that is 3 km wide and 250 m deep (A-A'). It has terraces with relative heights ranging from 100 to 200 m and well-developed arcuate scarps. Several knickpoints, can be observed along the main axis in this sector, which are points where a sudden change in the longitudinal gradient occurs. Additionally, a separate, less-incised proto-canyon is observed on the northern interfluve, although it is not connected to C1. The meandering segment of the shallow lower slope (Figure 4 B) displays a U-shaped profile that is 300 m deep and 3.5 km wide (B-B'). It is characterized by well-developed asymmetrical terraces. As the canyon reaches the

Journal Pre-proof

escarpment (Figure 4 C), it significantly widens and deepens (profile C-C'), reaching widths and depths of up to 4 km and 500 m, respectively.

Beyond the high-resolution data area, below 3200 mbsl, the morphology of the canyon can only be inferred from the coarser GEBCO data. In this region, a branch oriented in the west-east direction potentially connects to the northern wall of C1 (Br in Figure 4 C).

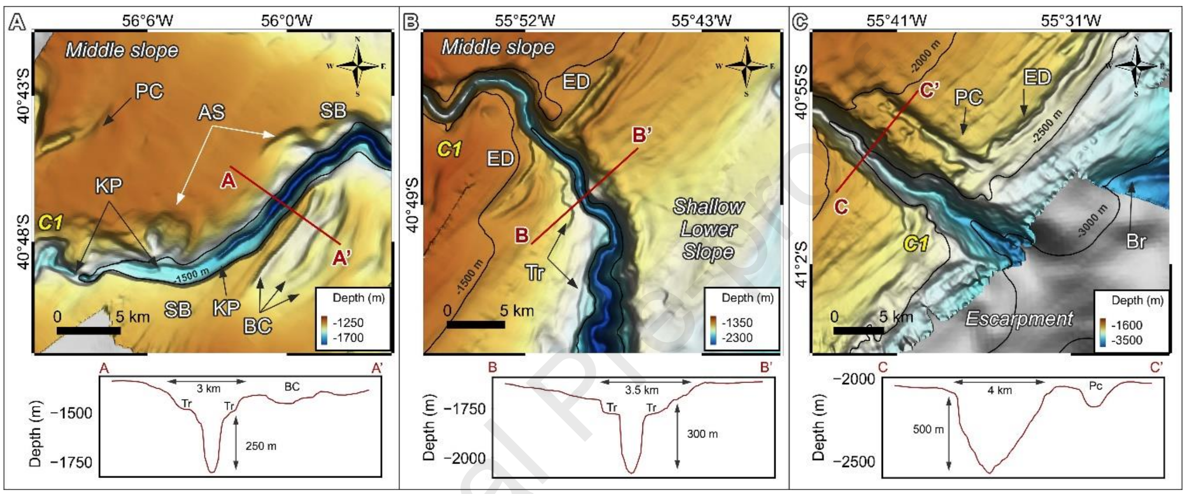

Figure 4: Bathymetric map of C1 and cross-sectional profiles along the thalweg. PC: Proto canyon. AS: Arcuate scarp. KP: Knickpoint. SB: Sharp bend. ED: Elongated depression. BC: Bedforms crests. Tr: Canyon terrace. Br: Canyon branch. The location of these figures is shown in Figure 2.

4.2.1.2 Canyon C2

C2 extends from 1322 to 4500 mbsl. It is characterized by a 125 km long thalweg, with a low sinuosity index (1.14). The canyon head cuts the middle slope with a valley that runs in a WNW-ESE direction (Figure 5 A) until ~1800 mbsl (Figure 5 B). Here, C2 makes a subtle bend, turning SW-NE for 10 km, and then changes again to a NW-SE direction, which it maintains until the escarpment (Figure 5 C).

C2 displays several cross-sectional changes along its thalweg. In the middle slope (Figure 5 A), the canyon valley is 70 m high with a wide (~5 km) U-shaped cross section and terraces (profile A-A’). At 1500 mbsl, two knickpoints mark the deepening and narrowing of the canyon to a 4 m wide and >200 m high valley (Figure 5 A). In the shallow lower slope, between 1600 and 1800 m (Figure 5 B), the canyon widens into a broad 7 km valley and bends to the SW-NE direction. The main valley recovers its previous orientation further deep water, displaying and a terraced morphology on the southeastern flank (B-B'). At the escarpment (Figure 5 C) the valley is 3 km wide and 200 m deep with a U-shaped profile (C-C'). This canyon shows the particularity of exhibiting a series of 20 and 60 m deep over-excavation ponds, subcircular depressions developed at the canyon floor not found in the other canyons here described. Downslope, at about 2800-3000 mbsl, the morphology of the canyon valley appears to be partially disrupted and only recovers a defined shape at water depths above 3000 m.

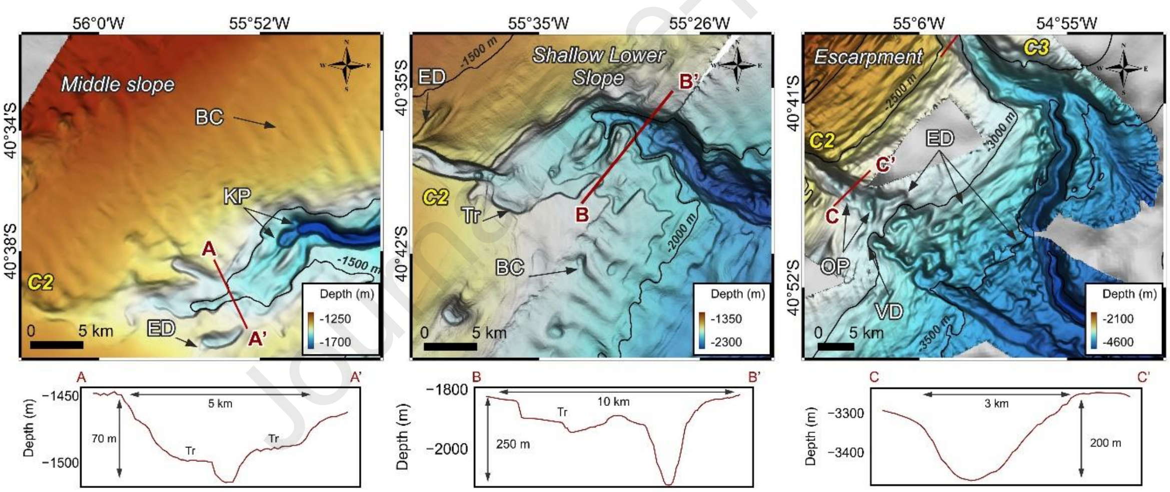

Figure 5: Bathymetric map of C2 and cross-sectional profiles along the thalweg. KP: Knickpoint. BC: Bedforms crests. ED: Elongated depression. Tr: Canyon terrace. OP: Over-excavation Pond. VD: Valley interruption/disruption. The location of these figures is shown in Figure 2.

4.2.1.3 Canyon C3

C3 extends over the entire continental slope, ranging from approximately 1000 to 5000 mbsl, with a total length of 239 km and a high sinuosity index of 1.39. In the upper and middle slope, the canyon predominantly follows a NW-SE orientation (Figure 6 A). However, its most distinctive feature is the

Journal Pre-proof

sharp bend that occurs in the shallow lower slope at approximately 1800 m. At this water depth, the valley turns to the NE, aligning with the regional isobaths for 21 km, before returning to a NW-SE orientation (Figure 6 B). When the escarpment merges with the upper continental rise, at 3500 m water depth, the canyon axis undergoes another bend, this time in a NE-SW direction (6 C). At 1500 mbsl, a large, irregularly shaped scarp runs along the transition from the Ewing Terrace to the lower slope (Figure 6 B). This scarp extends for 35 km following a SW-NE strike, which is parallel to the regional isobaths and the orientation assumed by the canyon in the same sector. The scarp stands at a height of 60 m and exhibits a dip of 22º.

Regarding its cross-sectional profiles, C3 exhibits two primary branches in the middle slope (Figure 6 A), each approximately 150 m deep and 2 km wide, featuring U-shaped profiles and a well-developed terrace on the southern walls (profile A-A'). These branches converge at 1400 mbsl, coinciding with two knickpoints situated upstream of the junction. In the shallow lower slope (Figure 6 B), the along-slope canyon valley shows an asymmetrical profile that spans 4 km in width and reaches a depth of 250 m (profile B-B'). In the escarpment, the canyon deepens and widens, forming a symmetrical V-shaped valley 8 km wide and 500 m deep (profile C-C').

Journal Pre-proof

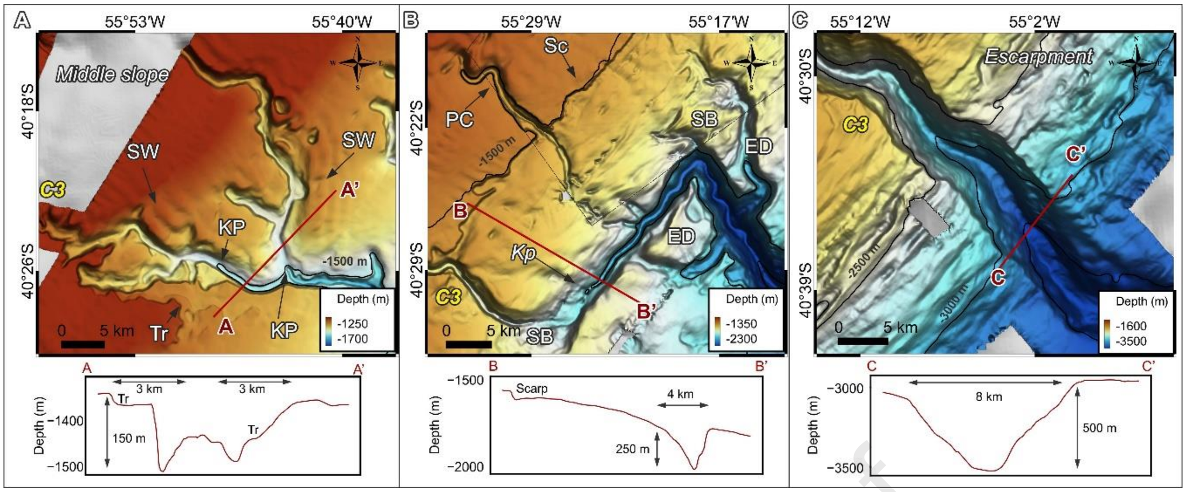

Figure 6: Bathymetric map of C3 and cross-sectional profiles along the thalweg. KP: Knickpoint. PC: Proto canyon. BC: Bedforms crests. ED: Elongated depression. Tr: Canyon terrace. Sc: Scarp. SB: Sharp bend. The location of these figures is shown in Figure 2.

4.2.1.4 Canyon C4

C4 develops between 900 and 3300 mbsl, spanning from the upper slope to the escarpment (Figure 7). It has a thalweg length of 129 km, a low sinuosity index (1.12) and runs mostly in the NW-SE direction, except for a subtle bend to the NE at 1500 m water depth. C4 has two main branches. The southern tributary, although only partially covered by the data, seems to originate in the upper slope as a single 1.5 km wide and 100 m deep valley (A-A'). In the middle slope, a 70 m high obstacle, located at 1300 mbsl, divides the canyon thalweg, which rejoins again 4 km further east. Downstream this bifurcation, the 120 m deep canyon displays an asymmetrical V-shaped profile with a very entrenched thalweg and a 7 km wide terrace developed on the southern wall (B-B'). Most of the northern branch lies outside the surveyed area and seems to be originated at the lower slope (C-C'). At 1800 mbsl it merges with the southern tributary forming a unique 1 km wide and 100 m deep channel that runs downslope until the escarpment (C-C').

Journal Pre-proof

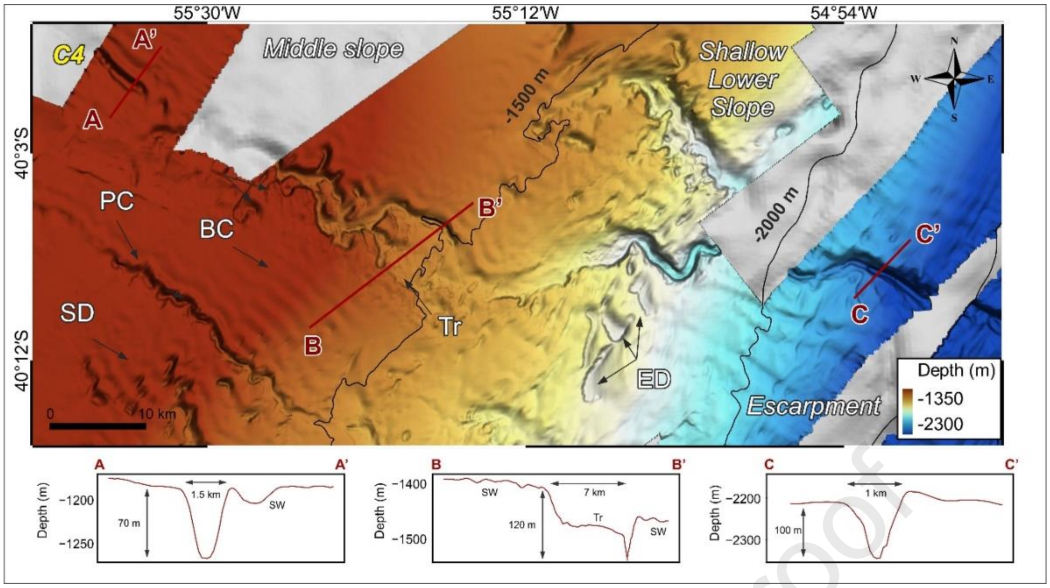

Figure 7: Bathymetric map of C4 and cross-sectional profiles along the thalweg. PC: Proto canyon. BC: Bedforms crests. ED: Elongated depression. SD: Sub-circular depression. Tr: Canyon terrace. The location of these figures is shown in Figure 2.

4.2.2 Depressions

Two categories of depressions can be distinguished according to their ellipticity index (EI). Of the total of 176 depressions identified in the study area, 114 are elongated (EI > 2) and 62 are subcircular (EI < 2).

The elongated depressions are oriented in the SW-NE NE with their major axis parallel to the bathymetric contours. These depressions display a broad spectrum of sizes, ranging from smaller ones with surface areas of 20 m^2, internal depths of 20 m, and elongated axis of 200 m, to much larger depressions covering extensive areas up to 35 km^2, internal depths of 160 m, and elongated axis stretching 16 km in length.

Some of them are situated between 1500 and 1800 mbsl and are connected to the walls of the canyons C1, C2 and C3 (Figure 4 B, Figure 5 B, Figure 6 B), while most of them are concentrated in the escarpment, between 2000 and 4200 m depth, giving this sector a rugged morphology. They can

Journal Pre-proof

be easily distinguished in the slope map by their regularly spaced stripes, featuring slope values greater than 10º (Figure 3).

The subcircular depressions have an average surface area of 2 km^2 (ranging from 0.5 to 3.5 km^2) and internal depth of 50 m (ranging from 10 to 150 m). They are predominantly observed in the middle slope area between the location of canyons C3 and C4 at 1400 mbsl (Figure 7).

4.2.3 Depositional features

Two distinct types of depositional bedforms with contrasting orientations can be observed in the study area.

The first type consists of extensive fields of longitudinal bedforms (LBF), with their crests oriented in the NW-SE direction, perpendicular to the bathymetric contours and the regional bottom currents (Figure 8). These bedforms are predominantly concentrated in the middle slope, ranging from 900 to 2000 mbsl. Table 1 represents a summary of their main morphometric parameters.

LBF1 (Figure 8 A) is located at the foot of the upper slope, between 900 and 1000 mbsl, and while it is not completely covered by the high-resolution data, it likely extends over an area of at least 2000 km^2, involving the entire inter-canyon area. It has wavelengths between 1800 and 3100 m and heights between 2.5 and 6.4 m, with slightly sinuous parallel crests. The cross profile shows an asymmetrical wave geometry, with their stoss side more developed than the lee side.

LBF2 (Figure 8 B) is located near the sharp bend of C1 with a profile that exhibits a downslope asymmetry toward the NE, wavelengths between 1060 and 1650 m and a mean height of 1.8 m. LBF3 (Figure 8 B) is a larger field associated with C2, that covers an area of 400 km^2. It displays a wide range of heights, from 0.5 to 4.5 m, and wavelengths between 1185 and 2100 m. LBF4 (Figure 8 C) is located downstream of the proto-canyon of the middle slope. It exhibits mostly symmetric crests with height values of up to 11 m and wavelengths that reach a maximum of 1491 m. LBF5

(Figure 8 C) extends over a wide area of at least 500 km^2 beyond the northern wall of C4 and represents a field with slightly asymmetric sinuous crests of small dimensions (1288 m and 2.7 mean wavelength and height respectively).

In the lower slope, these bedforms are only found at around 2000 mbsl in the vicinity of C2. LBF6 (Figure 8 D) is found near the sharp bend of C2 and displays the greatest crest heights the area, reaching values of up to 22.8 m. LBF7 (Figure 8 D) develops over a small area of 60 km^2 down water of C2, displaying downslope asymmetric sinuous crests towards the ENE direction, wavelengths between 1336 and 2209 m, and heights in the 3.9-6.4 m range.

Morphology	Depth range (m)	Minimum height (m)	Maximum height (m)	Mean height (m)	Minimum wavelength (m)	Maximum wavelength (m)	Mean wavelength (m)	Area (Km^2)
LBF1	900-1000	2.5	6.4	5.4	1800	3100	2477	2000
LBF2	1200-1400	1	4.9	1.8	1060	1650	1385	400
LBF3	1200-1400	0.5	4.5	1.8	1185	2100	1567	400
LBF4	1200-1600	4.3	11	8.1	1286	1491	1405	600
LBF5	1200-1600	0.1	5.8	2.7	948	2006	1288	500
LBF6	1900-2100	3.1	22.8	15.4	1495	2392	1971	150
LBF7	1900-2100	3.9	6.4	5.3	1336	2209	1872	60

Table 1: Morphometric parameters of the longitudinal bedforms represented in Figure 8

Journal Pre-proof

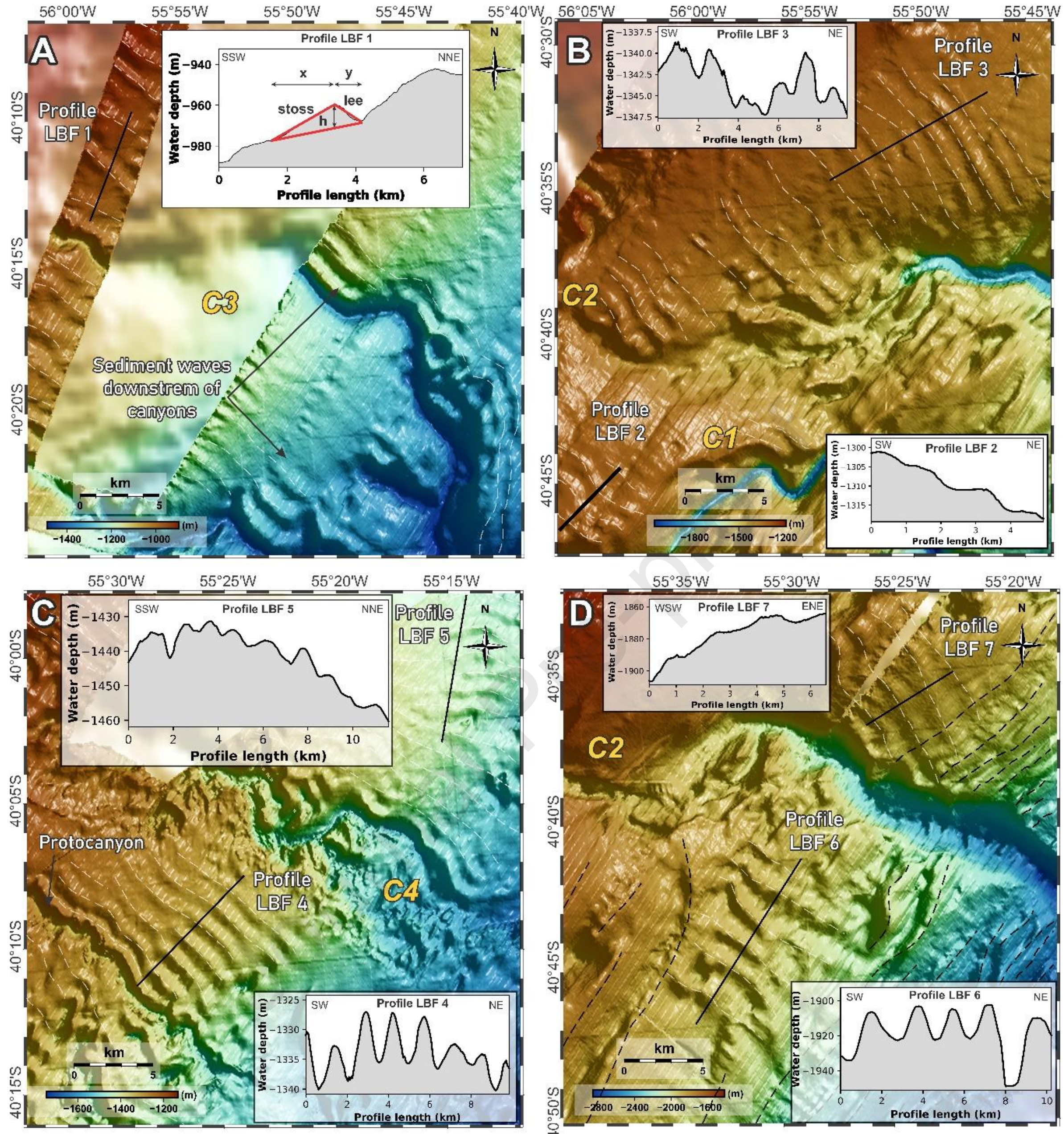

327

328 *Figure 8: Zoomed bathymetric sections of the different longitudinal bedform fields (LBF) of the study area (Vertical*
329 *exaggeration: ~15). Profile LBF1 also shows the geometric parameters taken from the grid to calculate the wavelength and*
330 *height of the waves. Cross sections depict the profiles at representative locations.*

331

332

The second type of depositional bedforms are found exclusively in the lower slope, where they follow a SW-NE direction, with their crests aligned parallel to the bathymetric contours and regional bottom currents, giving this domain a morphology characterized by a highly undulating topography (Figure 9 A). In the shallow lower slope, between 1500 and 2000 mbsl, these wavy bedforms cover the entire inter-canyon area. They exhibit an asymmetrical profile and reach an average height of 10 m, with wavelengths ranging from 1000 to 4000 m. At about 1900 mbsl, they interact with LBF6 and 7 (Figure 9 A). In the escarpment region, between 2000 and 4000 meters, on the contrary, the morphology of the waves shows a highly asymmetrical profile with prominent crests that reach heights between 20 and 40 m (Figure 9 A). The wavelengths are shorter than those observed on the shallow lower slope, ranging from 500 to 2000 m (Figure 9 B).

Journal Pre-proof

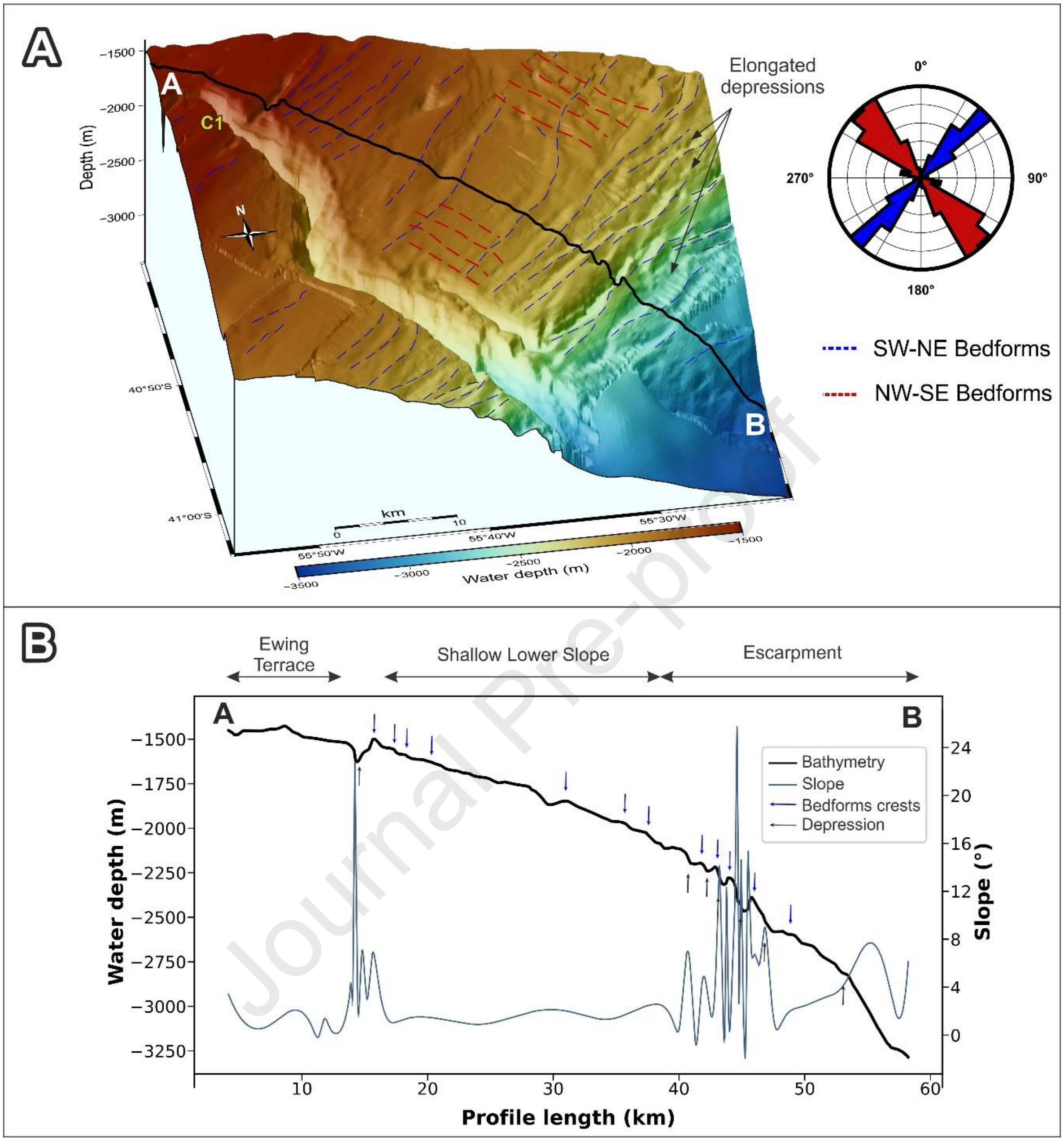

Figure 9: A: 3D perspective image of a sector of the escarpment, showing the interaction of the two types of wavy bedforms. The rose diagram represents their contrasting orientation. The black line denotes the profile of Sub-figure B. B: Double plot of water depth and slope along the slope parallel wavy bedforms.

5 Discussion

The bathymetric distribution of the geomorphological elements identified in the southern sector of the northern Argentinean continental slope reveals a complex present-day landscape (Figure 10). The principal factors that have been shaping this sector of the margin can be classify in two groups: 1) across-slope processes, characterized mainly by the presence of submarine canyons, and 2) along-slope processes, represented by erosive and depositional bedforms associated with the action of bottom current. By analyzing the high-resolution bathymetry, we gained an accurate comprehension of how these two processes interplay on the continental slope, a topic that will be discussed further in subsequent sections.

5.1 Processes affecting canyon morphology.

Based on the geometry and morphological characteristics of the four canyons examined in this study, we can draw some interpretations regarding the processes responsible for their evolution. The mechanisms acting behind the formation of submarine is a matter of debate, although most authors agree that their genesis is generally driven by two factors: 1) Slope failure, retrogressive erosion, and other mass wasting events. 2) Erosive turbidity flows originating from fluvial, shelf, and upper-slope (Farre et al., 1983; Harris and Whiteway, 2011; Pratson and Coakley, 1996).

The dominant processes in canyon formation are ultimately linked to their maturity state and their connection with external sources of sediment supply. According to the evolutionary model proposed by Farre et al. (1983) and Puga-Bernabéu et al. (2011) the formation of submarine canyons undergoes three distinct phases, involving the interaction of downslope and upslope processes. Remarkably, the study area presents visible examples of these phases.

In the initial youthful stages, canyons begin to take shape as minor incisions confined to the continental slope, often referred to as "proto-canyons". Various pre-conditioning factors can trigger

Journal Pre-proof

Journal Pre-proof

these initial stages, such as low sediment strength, differential compaction, sediment permeability, oversteepening, and the presence of faults and tectonic structures (de Almeida et al., 2015). These factors lead to localized slope failures and further retrogressive erosion (de Almeida et al., 2015; Lo Iacono et al., 2014; Puga-Bernabéu et al., 2011). In the escarpment sector, where failure and slumping events are frequent (Gruetzner et al., 2016) some of these processes appear to be actively shaping the development of proto-canyons (Figure 4 and Figure 10). On the middle slope, different formation processes seem to be at play, as several closely spaced depressions appear to amalgamate giving rise to a distinct type of proto-canyon (Figure 6B and Figure 7).

Over time, these incipient submarine canyons can progress into a transitional phase, evolving to connect and form a single channel, while the valley widens and deepens due to progressive slope failures and retrogressive erosion. These transitional canyons, referred to as "blind" and slope-confined canyons (Harris and Whiteway, 2011) remain disconnected from the shelf and typically exhibit low sinuosity (Farre et al., 1983). Examples of this transitional phase in canyon evolution can be seen in C2 and C4 (Figure 5 and Figure 7). Particularly, C2 appears to consist of three straight segments (Figure 5). The connection between the middle and lower slope segments seems to occur through an irregular and wide SW-NE section featuring several terraces (Figure 5B). The deepest sector of the canyon (Figure 5C) appears disconnected from its upslope segment, further indicating its youthful stage of evolution.

Despite being confined to the slope and lacking direct shelf sediment input, these canyons have the capacity to transport sediment along their channels. The frequent mass wasting processes during their evolution transform into turbiditic flows as they are channeled along the canyon axes (Talling, 2014). Consequently, these erosive currents could lead to the formation of over-excavated ponds within C2, similar to depressions observed in other submarine canyons of the Argentine Continental Margin (Lastras et al., 2011; Palma et al., 2021). These depressions likely result from the action of

Journal Pre-proof

vigorous along-canyon turbidity currents, which can effectively erode sediment from the canyon floor (Lastras et al., 2007). Moreover, C4 also appears to be in a transitional phase, characterized by a less incised bended portion that connects two straight and narrow segments, one upslope and the other downslope.

The mature stage involves a change in the erosion style of canyons that may reach the shelf edge (de Almeida et al., 2015) as is the case of C3 in the study area (Figure 6). Although these canyons have no direct connection with fluvial systems, sediment from the continental shelf can be delivered to canyons head and generate turbiditic flows that leave characteristic morphological imprints in the canyon morphology, like a highly sinuous thalweg (Farre et al., 1983). The morphological imprint of this erosive action exhibits variation across the slope, with cross-sectional profiles transitioning from V-shaped valleys on the middle slope to U-shaped profiles on the lower slope and escarpment sectors. These morphological changes likely indicate a predominant influence of erosive processes near the canyon head compared to the lower sector (Gerber et al., 2009; Mitchell, 2006; Palma et al., 2021).

Another frequent characteristic observed within the middle slope sector of C3 (Figure 6) is the presence of changes in the longitudinal gradient of the canyon floor, commonly known as knickpoints (Mitchell, 2006). These knickpoints result from changes in base level, tectonic uplift, lithological resistance (Mitchell, 2006) or the action of turbidity currents (Toniolo and Cantelli, 2007). They represent transitory states of equilibrium between canyon sectors (Tubau et al., 2015) suggesting that canyons within the middle slope are in a stage of adjustment to the new base level, possibly due to increasing turbidity current activity. Additionally, the observation of terraces, flat structures located several meters to tens of meters above the thalweg, provides additional evidence of significant changes in base level within the canyons (Mulder, 2011). Although the connection of C1 with the shelf is not visible in the study area (Figure 4), it shares the characteristics of a mature canyon, similar to C3, exhibiting a high sinuosity index, variations in cross-sectional profiles across the slope, and evidence of enhanced erosion towards the canyon head.

Furthermore, the most distinctive characteristic of these canyons system are their changes in orientation across the slope (Figure 2 and Figure 3). While most canyons typically align with the slope gradient, C2 and C3 exhibit oblique segments that run parallel to the SW-NE bathymetric contours (Figure 5 B and Figure 6 B). Similar morphologies have been observed in the Ameghino and Almirante Brown canyons located in the Patagonian margin (Bozzano et al., 2017; Ewing and Lonardi, 1971; Hernández-Molina et al., 2009). These patterns have been attributed to discontinuities inherited from Andean tectonics (Rossello et al., 2005), deflection of the main valleys by bottom currents (Hernández-Molina et al., 2009; Lastras et al., 2011), or a combination of both (Ewing and Lonardi, 1971). In the case of the canyons of the NACM, the morphological evidence suggests that the bends may be influenced by the action of along-slope currents, in line with the model proposed by Lastras et al. (2011) for the Patagonian Margin Canyons. These bends predominantly occur in the 1700-1800 m depth range, which coincides with the boundary layer between UCDW and LCDW. Water mass boundary layers are associated with enhanced bottom currents (Rebesco et al., 2014), which could contribute to the formation of the elongated depressions connected to the canyon walls (Figure 4 B). Over time, these depressions have the potential to evolve and expand in size under the influence of bottom currents and ultimately leading to directional changes in the canyon axes through the amalgamation of the elongated depressions with the canyon branches.

5.2 Morphological evidence of along-slope processes

The presence of a significant CDS along the NACM has been extensively documented in the recent literature of the study area (Ercilla et al., 2019; Gruetzner, 2014; Gruetzner et al., 2016, 2012; Hernández-Molina et al., 2009; Preu et al., 2013, 2012). Although a detailed analysis of the

Journal Pre-proof

morphosedimentary characteristics is beyond the scope of this work, some interesting features have been identified through this morpho bathymetric analysis that have enhanced previous interpretations that could be explored in further studies to understand the dynamics of this CDS.

One of them are the bedforms located mostly downstream of submarine canyons in the middle slope between 900 and 2000 mbsl, displaying crests aligned NW-SE, perpendicular to the slope trend and parallel to the axis of the canyons (Figure 8 and Figure 10). Their morphology and orientation are consistent with bottom current sediment waves, which often form large-scale fields covering extensive areas of the seafloor (Wynn and Stow 2002; Wynn and Masson 2008). The development of sediment waves, formed by the along slope action of the upper circumpolar deep water (UCDW) in the Ewing Terrace, has been documented in the study area (Ercilla et al., 2019) and other sectors of the NACM (Wilckens et al., 2021) through seismic data analysis.

An interesting aspect of these bedforms is their distribution along the downstream flank of submarine canyons. This observation suggests a potential interaction between the canyons and the bottom current, a common occurrence in mixed contourite-turbidite depositional systems (Rodrigues et al., 2022). In such systems, turbidity plumes from the submarine valleys are captured by bottom currents, leading to the redeposition of sediment waves on the downstream flank (Fonnesu et al., 2020; Mulder et al., 2008). At the water depths where these landforms occur, submarine canyons do not exceed a few hundred meters, which is a condition for the overspilling of turbiditic currents (Azpiroz-Zabala et al. 2017; Paull et al. 2018; Li et al. 2021), and further development of mixed deposits (Mencaroni et al., 2021). However, while the morphological characteristics suggest a potentially similar dynamic, a comprehensive sedimentological and seismic analysis is necessary to confirm this hypothesis.

Journal Pre-proof

Journal Pre-proof

Another type of depositional features are the wavy bedforms, which develop along the lower slope (Figure 9). These features form elongated bodies with their crests aligned SW-NE, parallel to the regional direction of the contour currents, located seaward of the boundary between the Upper Circumpolar Deep Water (UCDW) and Lower Circumpolar Deep Water (LCDW) water masses. Similar wavy bedforms have been found worldwide in marine settings. In the Mediterranean margin, comparable seafloor undulations in a prodeltaic environment were interpreted either as a product of the interaction of bottom currents with hyperpycnal flows (Urgeles et al., 2007) or as result of downslope sediment deformation (Urgeles et al., 1999). Different interpretations can be found in other settings characterized by strong bottom currents. Tallobre et al. (2016) for example, described similar along-slope parallel bedforms on the Demerara Plateau and interpreted them as longitudinal waves formed by the along-slope flow associated with the North Atlantic Deep Water Current. On the other hand, Wilckens et al. (2021) considered these types of landforms as contouritic sediment waves influenced by internal waves propagating at the interfaces of different water masses.

In this work, these features are interpreted as contourite drifts according to the model proposed by Preu et al. (2013) for this region, where plastered drifts develop seaward of contouritic terraces due to processes associated with water mass interfaces. Other authors have also identified the presence of contourites at these water depths (Hernández-Molina et al., 2009; Kirby et al., 2021; Rodrigues et al., 2022). Furthermore, Ercilla et al. (2019) have described these features in the study area using multichannel seismic profiles, and interpreted them as a complex drift, which can have locally a single or multi-crested morphology. Therefore, we refer to them as "multi-crested drifts" due to their widespread wavy morphology, which is similar to other contouritic bodies described in the literature (Haberkern, 2017; Miramontes et al., 2019, 2016).

Furthermore, the bathymetry reveals the presence of several depressions that may be associated with the erosive action of bottom currents. Some of these depressions, observed in the Ewing

Journal Pre-proof

Terrace (Figure 7), appear to merge, forming more complex crescent shapes. Such scouring patterns are indicative of marine environments with strong bottom-current activity, as documented in the Iberian Peninsula (Glazkova et al., 2022), the Sète canyon (Lastras et al., 2007) and the Patagonian Margin (Lastras et al., 2011; Muñoz et al., 2013).

The concentration of elongated depressions between 2000 and 4000 mbsl is likely not coincidental. Previous studies have identified a subsurface fault system of gravitational origin at these water depths (Anka et al., 2014; Loegering et al., 2013, figure 2), that affects the majority of tertiary sedimentary column and results in a disrupted seafloor featuring several scarps identified in seismic profiles (Gruetzner et al., 2016). Although these seaward dipping faults do not appear to outcrop, these buried structures seem to play a substantial role in shaping the rugged topography of the escarpment, marked by its steep slope. It has been proposed that bottom current flow may concentrate along linear features like fault scarps, thereby enhancing erosion and broadening the pre-existing topography (Krastel et al., 2011), and forming contour parallel elongated depressions as those described in this work. These types of scouring are typically associated with erosional contourite environments and are considered high-energy ambient bedforms, with flow velocities ranging from tens of decimeters to meters per second, depending on the seafloor lithology (Stow et al., 2009; Wynn and Masson, 2008).

Although direct measurements of bottom current velocity are lacking, the identification of these current-derived features provides valuable clues about the different flow regimes in the study area. These observations could serve as a promising starting point for reconstructing the bottom-current flow in this sector of the slope.

Journal Pre-proof

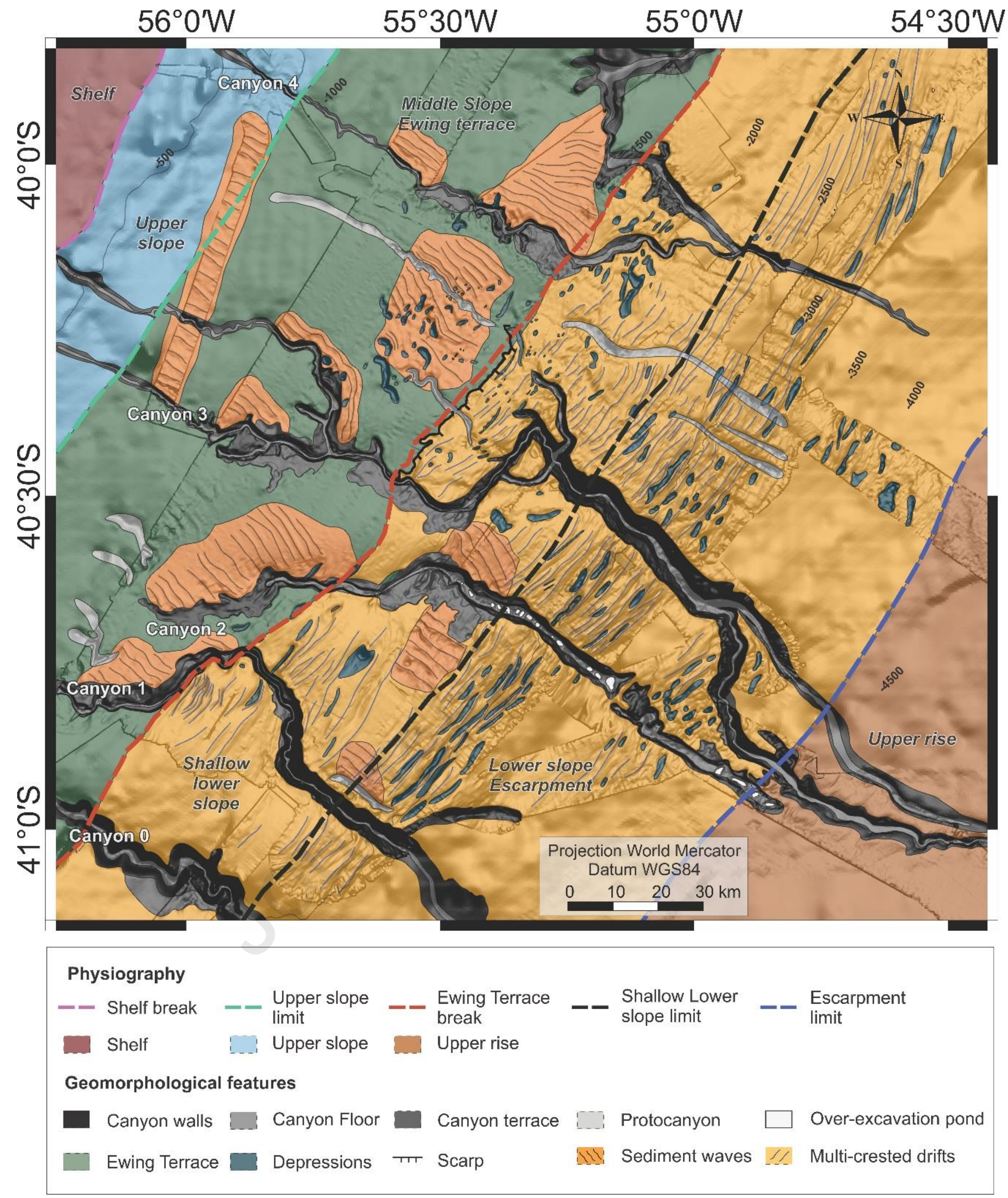

Figure 10: Geomorphological map of the northern Argentine continental slope at 40-41º S

6 Conclusions

This study represents a significant advancement in understanding the geomorphological characteristics of the previously unmapped southern sector of the northern Argentine continental margin (NACM). By utilizing high-resolution multibeam data and 3D seismic-derived bathymetry, we conducted a detailed analysis of the seafloor features in this region. Our findings revealed a diverse array of seafloor features, providing evidence of different sedimentary processes shaping the continental slope, that can be summarized as follows:

I. We identified four complex submarine canyons extending through the whole study area between 900 and 5000 mbsl. that display excellent examples of different stages of evolution. The young stages are represented by the minor incisions found in the middle slope and escarpment, which are interpreted as proto-canyons; the blind canyons C2 and C4, approximately 100 km long, represent transitional phases of evolution; finally, the mature stage is exemplified by canyon C3, a large 239 km long canyon connected to the continental shelf.

II. Erosive features, such as sub-circular and elongated depressions, were also observed, indicating periods of enhanced bottom current activity, and scouring of the slope. Some coalescent sub-circular depressions appear to be actively interacting with the submarine canyons, favoring the formation of proto-canyons in the middle slope at 1400 mbsl, while those with an elongated morphology appear to give rise to the bended sections further deep water between 1500 and 1800 mbsl in the transition to the lower slope.

III. Two types of depositional bedforms were identified in the study area. Sediment waves are concentrated in the middle slope in water depths ranging from 900 to 2000 mbsl, forming extensive fields of 400-500 km^2 along the downstream flank of the canyons Their preferential location as well as their crest alignment perpendicular to the regional current, suggests a possible interplay between bottom currents and the dynamics related to the submarine

Journal Pre-proof

canyons. Additionally, multicrested contourite drifts, with their crest parallel to the bathymetric contours, were found covering the inter-canyon area in the lower slope between 1500 and 4000 mbsl. These bedforms contribute to the overall wavy morphology of the lower slope and appear to be a product of the interaction between bottom currents and seafloor morphology.

Finally, the insights gained from this research contribute to a better understanding of the geological and oceanographic processes in the region and serve as a reference point for future studies regarding the Quaternary evolution of the continental slope, paleoceanographic history of the western South Atlantic and deep-sea sedimentary processes.

Acknowledgements

The authors are grateful to the Argentine Hydrographic Survey (SHN) as well as the captain, officials, and crew of the R/V Austral for their dedication during the 'YTEC-GTGM 4' cruises. We also express our gratitude to the Argentine Ministry of Energy and Mining (MINEN) for providing us the 'Colorado 3D' seismic data used in this work. We sincerely appreciate the work done during the cruise by the members of the Marine Geology Working Group (Edgardo Monteros, Eloy Mendoza, Fernando Almaraz, Yasmin Gutierrez, Daniela Spoltore and Cesar Artunduaga). The authors thank Nestor Bolatti and the YPF S.A. offshore team for their constant support. Finally, we extend our thanks to the editor, Dr Andrés Folguera, and the anonymous reviewer for their insightful comments, which significantly enhanced the manuscript's quality.

Funding

This research is framed within a collaborative project between YPF-Technology (Y-TEC) and the National Scientific and Technical Research Council (CONICET), designed to manage the efforts related to the study of the Argentine offshore territory. In addition, this work was partly funded by the CONICET research project 2021-2023 11220200103152CO (SIMOCA) and the Pampa Azul Research and Technological Development Project RE-2021-68428463-APN-DDYGD#MCT 2022-2024 (GeoFMRP).

References

Anka, Z., Loegering, M.J., di Primio, R., Marchal, D., Rodríguez, J.F., Vallejo, E., 2014. Distribution and origin of natural gas leakage in the Colorado Basin, offshore Argentina Margin, South America: seismic interpretation and 3D basin modelling. Geologica Acta 12, 269–285.

Azpiroz-Zabala, M., Cartigny, M.J.B., Talling, P.J., Parsons, D.R., Sumner, E.J., Clare, M.A., Simmons, S.M., Cooper, C., Pope, E.L., 2017. Newly recognized turbidity current structure can explain prolonged flushing of submarine canyons. Sci Adv 3.

Bozzano, G., Martín, J., Spoltore, D. V., Violante, R.A., 2017. Los cañones submarinos del margen continental argentino: Una síntesis sobre su génesis y dinámica sedimentaria. Latin American Journal of Sedimentology and Basin Analysis 24, 85–101.

Charlton, R., 2007. Fundamentals of fluvial geomorphology. Routledge.

Daly, R.A., 1936. Origin of submarine canyons. Am J Sci 5, 401–420.

de Almeida, N.M., Vital, H., Gomes, M.P., 2015. Morphology of submarine canyons along the continental margin of the Potiguar Basin, NE Brazil. Mar Pet Geol 68, 307–324.

Ercilla, G., Schwenk, T., Bozzano, G., Spiess, V., Violante, R., Estrada, F., Ianniccheri, F., Spoltore, D. V., Alonso, B., 2019. Cenozoic sedimentary history of the northern Argentine continental slope, off Bahia Blanca, the location of the Ewing Terrace: Palaeogeodynamic and palaeoceanographic implications. Mar Geol 417, 106028.

Journal Pre-proof

Ewing, M., Lonardi, A.G., 1971. SEDIMENT TRANSPORT AND DISTRIBUTION IN THE ARGENTINE BASIN: SEDIMENTARY STRUCTURE OF THE ARGENTINE MARGIN, BASIN, AND RELATED PROVINCES. Physics and Chemistry of the Earth 8, 125–156.

Farran, M., 2008. IMAGE2SEGY: Una aplicación informática para la conversión de imágenes de perfiles sísmicos a ficheros en formato SEG Y. Geo-Temas 1–4.

Farre, J.A., McGregor, B.A., Ryan, W.B.F., Robb, J.M., 1983. Breaching the shelfbreak: passage from youthful to mature phase in submarine canyon evolution. In: The Shelfbreak: Critical Interface on Continental Margins. SEPM (Society for Sedimentary Geology), pp. 25–39.

Fernandez-Arcaya, U., Ramirez-Llodra, E., Aguzzi, J., Allcock, A.L., Davies, J.S., Dissanayake, A., Harris, P., Howell, K., Huvenne, V.A.I., Macmillan-Lawler, M., others, 2017. Ecological role of submarine canyons and need for canyon conservation: a review. Front Mar Sci 4, 5.

Fonnesu, M., Palermo, D., Galbiati, M., Marchesini, M., Bonamini, E., Bendias, D., 2020. A new world-class deep-water play-type, deposited by the syndepositional interaction of turbidity flows and bottom currents: The giant Eocene Coral Field in northern Mozambique. Mar Pet Geol 111, 179–201.

Gavazzi, G.M., 2019. Development of seafloor mapping strategies supporting integrated marine management Development of seafloor mapping strategies supporting integrated marine management Application of seafloor backscatter by multibeam echosounders 2018–2019.

GEBCO Bathymetric Compilation Group 2021, 2021. The GEBCO_2021 Grid - a continuous terrain model of the global oceans and land.

Gerber, T.P., Amblas, D., Wolinsky, M.A., Pratson, L.F., Canals, M., 2009. A model for the long-profile shape of submarine canyons. J Geophys Res Earth Surf 114, 1–24.

Glazkova, T., Hernández-Molina, F.J., Dorokhova, E., Mena, A., Roque, C., Rodríguez-Tovar, F.J., Krechik, V., Kuleshova, L., Llave, E., 2022. Sedimentary processes in the Discovery Gap (Central–NE Atlantic): An example of a deep marine gateway. Deep Sea Res 1 Oceanogr Res Pap 180.

Gruetzner, J., 2014. Slowdown of Circumpolar Deepwater flow during the Late Neogene: Evidence from a mudwave field at the Argentine continental slope. Geophys Res Lett 6413–6419.

Gruetzner, J., Uenzelmann-Neben, G., Franke, D., 2012. Variations in sediment transport at the central Argentine continental margin during the Cenozoic. Geochemistry, Geophysics, Geosystems 13, 1–15.

Gruetzner, J., Uenzelmann-Neben, G., Franke, D., 2016. Evolution of the northern Argentine margin during the Cenozoic controlled by bottom current dynamics and gravitational processes. Geochemistry Geophysics Geosystems 17, 1312–1338.

Haberkern, J., 2017. Contouritic depositional systems influenced by complex seafloor topography : Late Cenozoic seismoacoustic reconstructions from the Galicia and Angola Continental Margins.

Harris, P.T., Whiteway, T., 2011. Global distribution of large submarine canyons: Geomorphic differences between active and passive continental margins. Mar Geol 285, 69–86.

Hernández-Molina, F.J., Paterlini, M., Somoza, L., Violante, R., Arecco, M.A., de Isasi, M., Rebesco, M., Uenzelmann-Neben, G., Neben, S., Marshall, P., 2010. Giant mounded drifts in the Argentine Continental Margin: Origins, and global implications for the history of thermohaline circulation. Mar Pet Geol 27, 1508–1530.

Journal Pre-proof

Hernández-Molina, F.J., Paterlini, M., Violante, R., Marshall, P., de Isasi, M., Somoza, L., Rebesco, M., 2009. Contourite depositional system on the Argentine slope: An exceptional record of the influence of Antarctic water masses. Geology 37, 507–510.

Isola, J.I., Bravo, M.E., Bozzano, G., Palma, F.I., Ormazabal, J.P., Principi, S., Spoltore, D., Martin, R., Esteban, F.D., Tassone, A.A., 2021. The Late-Quaternary deposits of the Piedra Buena Terrace (Patagonian continental slope, SW Atlantic): An example of interaction between bottom currents and seafloor morphology. Mar Geol.

Kirby, A., Javier, F., Molina, H., Rodrigues, S., 2021. Lateral migration of large sedimentary bodies in a deep - marine system offshore of Argentina. Sci Rep 1–10.

Krastel, S., Wefer, G., Hanebuth, T.J.J., Antobreh, A.A., Freudenthal, T., Preu, B., Schwenk, T., Strasser, M., Violante, R., Winkelmann, D., 2011. Sediment dynamics and geohazards off Uruguay and the de la Plata River region (northern Argentina and Uruguay). Geo-Marine Letters 31, 271–283.

Lastras, G., Acosta, J., Muñoz, A., Canals, M., 2011. Submarine canyon formation and evolution in the Argentine Continental Margin between 44°30’S and 48°S. Geomorphology 128, 116–136.

Lastras, G., Canals, M., Urgeles, R., Amblas, D., Ivanov, M., Droz, L., Dennielou, B., Fabrés, J., Schoolmeester, T., Akhmetzhanov, A., Orange, D., García-García, A., 2007. A walk down the Cap de Creus canyon, Northwestern Mediterranean Sea: Recent processes inferred from morphology and sediment bedforms. Mar Geol 246, 176–192.

Li, W., Li, S., Alves, T.M., Rebesco, M., Feng, Y., 2021. The role of sediment gravity flows on the morphological development of a large submarine canyon (Taiwan Canyon), north-east South China Sea. Sedimentology 68, 1091–1108.

Journal Pre-proof

Lo Iacono, C., Sulli, A., Agate, M., 2014. Submarine canyons of north-western Sicily (Southern Tyrrhenian Sea): Variability in morphology, sedimentary processes and evolution on a tectonically active margin. Deep Sea Res 2 Top Stud Oceanogr 104, 93–105.

Loegering, M.J., Anka, Z., Autin, J., di Primio, R., Marchal, D., Rodriguez, J.F., Franke, D., Vallejo, E., 2013. Tectonic evolution of the Colorado Basin, offshore Argentina, inferred from seismo-stratigraphy and depositional rates analysis. Tectonophysics 604, 245–263.

Mencaroni, D., Urgeles, R., Camerlenghi, A., Llopart, J., Ford, J., Sanchez Serra, C., Meservy, W., Gràcia, E., Rebesco, M., Zitellini, N., 2021. A mixed turbidite – contourite system related to a major submarine canyon: The Marquês de Pombal Drift (south-west Iberian margin). Sedimentology 2069–2096.

Michel, G., Ehrhold, A., Scalabrin, C., Imbert, P., Pitel, M., Geldof, J., Lazure, P., Marie, L., 2017. Pockmarks on the South Aquitaine Margin continental slope: The seabed expression of past fluid circulation and former bottom currents. Comptes Rendus Geoscience 349, 391–401.

Miramontes, E., Cattaneo, A., Jouet, G., Théreau, E., Thomas, Y., Rovere, M., Cauquil, E., Trincardi, F., 2016. The Pianosa Contourite Depositional System (Northern Tyrrhenian Sea): Drift morphology and Plio-Quaternary stratigraphic evolution. Mar Geol 378, 20–42.

Miramontes, E., Garreau, P., Caillaud, M., Jouet, G., Pellen, R., Hernández-Molina, F.J., Clare, M.A., Cattaneo, A., 2019. Contourite distribution and bottom currents in the NW Mediterranean Sea: Coupling seafloor geomorphology and hydrodynamic modelling. Geomorphology 333, 43–60.

Mitchell, N.C., 2006. Morphologies of knickpoints in submarine canyons. Bulletin of the Geological Society of America 118, 589–605.

Journal Pre-proof

Mulder, T., 2008. Chapter 2: Gravity processes and deposits on continental slope, rise and abyssal plains, 1st ed, Developments in Sedimentology. Heiko Hneke and Thierry Mulder.

Mulder, T., Faugères, J.C., Gonthier, E., 2008. Chapter 21 Mixed Turbidite-Contourite Systems. Developments in Sedimentology 60, 435–456.

Muñoz, A., Acosta, J., Cristobo, J., Druet, M., Uchupi, E., Iglesias, S., Portela, J., Del Río, J.L., Parra, S., Sacau, M., Vilela, R., Patrocinio, T., Ríos, P., Almón, B., Elvira, E., Jiménez, P., Fontán, A., Alcalá, C., López, V., 2013. Geomorphology and shallow structure of a segment of the Atlantic Patagonian margin. Earth Sci Rev 121, 73–95.

Palma, F.I., Bozzano, G., Principi, S., Isola, J.I., Ormazabal, J.P., Esteban, F.D., Tassone, A.A., 2021. Geomorphology and sedimentary processes on the Sloggett Canyon, Northwestern Scotia Sea, Argentina. J South Am Earth Sci.

Paull, C.K., Talling, P.J., Maier, K.L., Parsons, D., Xu, J., Caress, D.W., Gwiazda, R., Lundsten, E.M., Anderson, K., Barry, J.P., Chaffey, M., O'Reilly, T., Rosenberger, K.J., Gales, J.A., Kieft, B., McGann, M., Simmons, S.M., McCann, M., Sumner, E.J., Clare, M.A., Cartigny, M.J., 2018. Powerful turbidity currents driven by dense basal layers. Nat Commun 9, 1–9.

Piola, A.R., Matano, R.P., 2001. Brazil And Falklands (malvinas) Currents, Earth Systems and Environmental Sciences. Elsevier Inc.

Power, H.E., Clarke, S.L., 2019. 3D seismic-derived bathymetry: a quantitative comparison with multibeam data. Geo-Marine Letters 39, 447–467.

Pratson, L.F., Coakley, B.J., 1996. A model for the headward erosion of submarine canyons induced by downslope-eroding sediment flows. Bulletin of the Geological Society of America 108, 225–234.

Journal Pre-proof

Preu, B., Hernández-Molina, F.J., Violante, R., Piola, A.R., Paterlini, C.M., Schwenk, T., Voigt, I., Krastel, S., Spiess, V., 2013. Morphosedimentary and hydrographic features of the northern Argentine margin: The interplay between erosive, depositional and gravitational processes and its conceptual implications. Deep Sea Res 1 Oceanogr Res Pap 75, 157–174.

Preu, B., Schwenk, T., Hernández-Molina, F.J., Violante, R., Paterlini, M., Krastel, S., Tomasini, J., Spieß, V., 2012. Sedimentary growth pattern on the northern Argentine slope: The impact of North Atlantic Deep Water on southern hemisphere slope architecture. Mar Geol 329–331, 113–125.

Puga-Bernabéu, Á., Webster, J.M., Beaman, R.J., Guilbaud, V., 2011. Morphology and controls on the evolution of a mixed carbonate-siliciclastic submarine canyon system, Great Barrier Reef margin, north-eastern Australia. Mar Geol 289, 100–116.

Ramos, V.A., 1996. Evolución tectónica de la Plataforma Continental. Geología y recursos naturales de la Plataforma Continental Argentina 21, 405–422.

Rebesco, M., Hernández-Molina, F.J., Van Rooij, D., Wåhlin, A., 2014. Contourites and associated sediments controlled by deep-water circulation processes: State-of-the-art and future considerations. Mar Geol 352, 111–154.

Reid, J., Nowlin, W., Patzert, W., 1977. On the Characteristics and Circulation of the Southwestern Atlantic Ocean. J Phys Oceanogr.

Rodrigues, S, Hernandez-Molina, F.J., Fonnesu, M., Miramontes, E., Rebesco, M., Campbell, D.C., 2022. A new classification system for mixed (turbidite-contourite) depositional systems: Examples, conceptual models and diagnostic criteria for modern and ancient records. Earth Sci Rev.

Journal Pre-proof

Rodrigues, S., Hernández-Molina, F.J., Larter, R.D., Rebesco, M., Hillenbrand, C.D., Lucchi, R.G., Rodríguez-Tovar, F.J., 2022. Sedimentary model for mixed depositional systems along the Pacific margin of the Antarctic Peninsula: Decoding the interplay of deep-water processes. Mar Geol 445.

Rossello, E.A., Lagabrielle, Y., Cobbold, P.R., Marshall, P., 2005. Los cañones submarinos oblicuos del talud continental argentino (40° a 45° S): evidencias de inversión tectónica andina sobre el margen pasivo atlántico? In: X Simposio Nacional de Estudos Tectónicos-IV International Symposium on Tectonics. pp. 90–93.

Schattner, U., 2016. Pockmark asymmetry and seafloor currents in the Santos Basin offshore Brazil. Geo-Marine Letters.

Shapiro, M., Shapiro, Michael, Shapiro, M., Shapiro, Michael, 2019. GRASS GIS manual: r.neighbors.

Shepard, F.P., 1972. Submarine canyons. Earth Science Reviews 8, 1–12.

Shepard, F.P., 1981. Submarine canyons: multiple causes and long-time persistence. American Association of Petroleum Geologists Bulletin 65, 1062–1077.

Steinmann, L., Baques, M., Wenau, S., Schwenk, T., Spiess, V., Piola, A.R., Bozzano, G., Violante, R., Kasten, S., 2020. Discovery of a giant cold-water coral mound province along the northern Argentine margin and its link to the regional Contourite Depositional System and oceanographic setting. Mar Geol 427, 106223.

Stow, D.A.V., Hernández-Molina, F.J., Llave, E., Sayago-Gil, M., Díaz-del Río, V., Branson, A., 2009. Bedform-velocity matrix: The estimation of bottom current velocity from bedform observations. Geology 37, 327–330.

Journal Pre-proof

Talling, P.J., 2014. On the triggers, resulting flow types and frequencies of subaqueous sediment density flows in different settings. Mar Geol 352, 155–182.

Tallobre, C., Loncke, L., Bassetti, M.A., Giresse, P., Bayon, G., Buscail, R., de Madron, X.D., Bourrin, F., Vanhaesebroucke, M., Sotin, C., 2016. Description of a contourite depositional system on the Demerara Plateau: Results from geophysical data and sediment cores. Mar Geol 378, 56–73.

Toniolo, H., Cantelli, A., 2007. Experiments on upstream-migrating submarine knickpoints. Journal of Sedimentary Research 77, 772–783.

Tubau, X., Paull, C.K., Lastras, G., Caress, D.W., Canals, M., Lundsten, E., Anderson, K., Gwiazda, R., Amblas, D., 2015. Submarine canyons of Santa Monica Bay, Southern California: Variability in morphology and sedimentary processes. Mar Geol 365, 61–79.

Urgeles, R., De Mol, B., Liquete, C., Canals, M., De Batist, M., Hughes-Clarke, J.E., Amblàs, D., Arnau, P.A., Calafat, A.M., Casamor, J.L., Centella, V., De Rycker, K., Fabrés, J., Frigola, J., Lafuerza, S., Lastras, G., Sànchez, A., Zuñiga, D., Versteeg, W., Willmott, V., 2007. Sediment undulations on the Llobregat prodelta: Signs of early slope instability or sedimentary bedforms? J Geophys Res Solid Earth 112, 1–12.

Urgeles, R., Masson, D.G., Canals, M., Watts, A.B., Le Bas, T., 1999. Recurrent large-scale landsliding on the west flank of La Palma, Canary Islands. J Geophys Res Solid Earth 104, 25331–25348.

Warratz, G., Henrich, R., Voigt, I., Chiessi, C.M., Kuhn, G., Lantzsch, H., 2017. Deglacial changes in the strength of deep southern component water and sediment supply at the Argentine continental margin. Paleoceanography 32, 796–812.

Journal Pre-proof

Wilckens, H., Miramontes, E., Schwenk, T., Artana, C., Zhang, W., Piola, A.R., Baques, M., Provost, C., Hernández-Molina, F.J., Felgendreher, M., Spieß, V., Kasten, S., 2021. The erosive power of the Malvinas Current: Influence of bottom currents on morpho-sedimentary features along the northern Argentine margin (SW Atlantic Ocean). Mar Geol 439.

Wynn, R.B., Masson, D.G., 2008. Chapter 15 Sediment Waves and Bedforms. Developments in Sedimentology 60, 289–300.

Wynn, R.B., Stow, D.A.V., 2002. Classification and characterisation of deep-water sediment waves. Mar Geol 192, 7–22.

Journal Pre-proof

Highlights:

•Geomorphology of a previously unmapped sector of the Argentine continental margin

•Combination of multibeam and 3D seismic-derived bathymetry for high resolution morphometric analysis.

•Description of diverse seafloor bedforms, current derived features and submarine canyons.

Journal Pre-proof

Declaration of interests

☒ The authors declare that they have no known competing financial interests or personal relationships that could have appeared to influence the work reported in this paper.

☐ The authors declare the following financial interests/personal relationships which may be considered as potential competing interests:

Journal Pre-proof